

E-ELT Primary Mirror Control System

M. Dimmler, T. Erm, B. Bauvir, B. Sedghi, H. Bonnet, M. Müller and A. Wallander
European Southern Observatory, Karl-Schwarzschild-Str. 2, 85748 Garching bei München,
Germany

ABSTRACT

During the past year the control of the 42m segmented primary mirror of the E-ELT has been studied. This paper presents the progress in the areas of M1 figure control and control hardware implementation. The critical issue of coupling through the supporting structure has been considered in the controller design. Different control strategies have been investigated and from a tradeoff analysis modal control is proposed as a solution addressing the topics of wind rejection as well as sensor noise in the presence of cross-coupling through the supporting structure. Various implementations of the M1 Control System have been studied and a centralized architecture has been selected as baseline. This approach offers maximum flexibility for further iterations. The controller design and main parts of the control system are described.

Keywords: wind rejection, edge sensor noise, figure control, modal control

1. INTRODUCTION

The Primary Mirror (M1) of the E-ELT has a diameter of 42m and consists of 984 quasi-hexagonal segments with a circumscribed diameter of 1.4 m. Each segment is connected to the backstructure by means of an axial support system consisting of three whiffle trees and three position actuators (PACT). The backstructure consists of several layers of framework structures with high local stiffness. The PACTs are used to control the out-of-plane motions piston, tip and tilt (PTT). Edge sensors (ES) are used to measure variations of the relative height between two neighboring segments. Two ES per edge are used. Furthermore warping harnesses built in to the whiffle trees are used to correct the shape of segments.

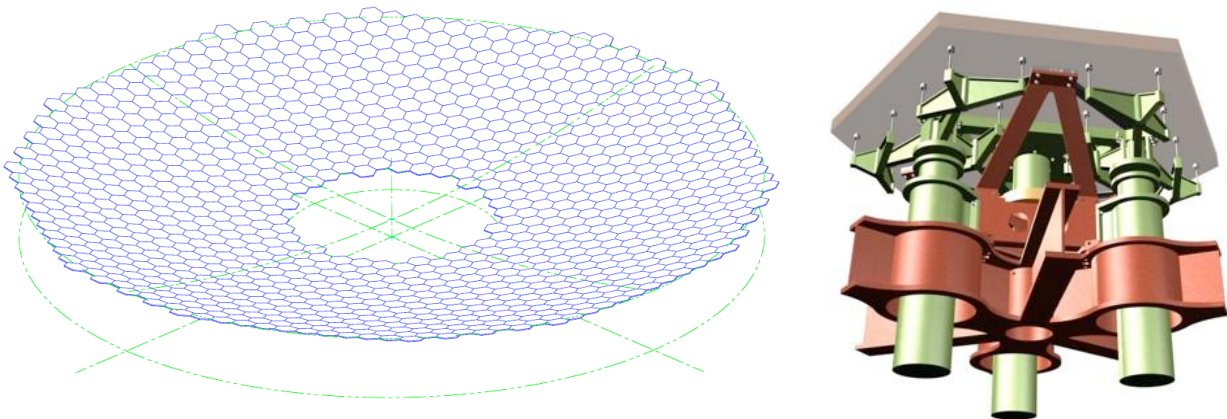


Fig. 1 M1 Layout with 984 segments (left), Subcell with 3 position actuators (right)

The M1 Control System (MICS) must support the following main functions:

- M1 figure control
- Segment shape control
- Phasing procedure

- Failure Detection, Isolation and Recovery (FDIR)
- Segment integration

This paper is focused on the evaluation of control strategies for the M1 figure control in the presence of disturbances and interaction between the segments introduced by the flexibility of the backstructure. The objective was to find a control strategy that delivers the required performance and can be efficiently implemented. The work has been supported by time-domain simulations using a dynamical model of the system. Another main driver for this work is to determine requirements and performance characteristics of the critical components of the MICS.

In parallel a survey of technologies and architectures has been made together with benchmarking of a potential solution for the implementation of the M1 Global Controller (M1GC). A first baseline has been selected, which will be presented in the following chapters.

2. CONTROL OBJECTIVES AND ASSUMPTIONS

2.1 Control objective

M1 figure control is responsible for maintaining the alignment of the 984 mirror segments to a level acceptable by the adaptive optics systems (telescope or post focal) in the presence of disturbances. The analysis has concentrated on finding the best control strategy that fulfills the performance requirement of 10 nm RMS wavefront after AO correction.

2.2 Assumptions

Various disturbances (internal and external) and noise sources are acting on the system and they are briefly described below together with assumptions used to model them. The main influences considered in the analysis are wind buffeting and ES noise.

Wind disturbance

The E-ELT reference wind load case on the Primary Mirror is based on a von Karman spectrum with the assumptions that the deviations from mean wind speed are small and that the wind speed field is isotropic and moved over the M1 at constant speed. The following parameters were used:

Wind speed $V_{wind} = 1.7$ m/s, turbulence Intensity $I = 0.4$ and outer scale $L = 7$ m.

Edge Sensor

For the purpose of dynamic studies, the ES are modeled as ideal sensors (i.e. only sensitive displacement along the direction normal to the segment optical surface) with the addition of uncorrelated white noise with a level of $0.2 \text{ nm}/\sqrt{\text{Hz}}$. These values are derived from the inductive edge sensor prototype developed during earlier studies.

Position actuator stiffness

The PACT was modeled as a pure stiffness lumped together with the stiffness of the whiffle tree. The analysis has been conducted in a way to determine the stiffness requirement rather than trying to specify the desired solution for implementation of the PACTs.

Vibrations

It is anticipated that the primary mirror will be exposed to narrow band vibrations in the frequency range of 10Hz to 60Hz mainly from rotating machinery of the observatory. No estimates for the disturbance force amplitudes are available yet. Therefore, vibrations have not been considered in the context of this study.

Telescope elevation

The analysis presented in this paper is performed at a fixed elevation.

Interaction matrix

The Control Matrix is derived from the Interaction Matrix (IM) between the PACT and ES. Deviations from the nominal geometrical sensitivity induced by changing gravity and thermal load or by mounting errors have not been considered.

AO rejection

The wavefront residual after the M1 figure control system is further corrected by the adaptive optics of the telescope. We used a simple linear model for the AO system: the static fitting error of the adaptive mirror on a mode of the PACT to ES IM is proportional to the singular value of the mode. The dynamic rejection is the ideal closed loop sensitivity function of a pure integrator running at 500Hz sampling rate with a gain of 0.5. The combination of the static fitting error with the dynamic rejection law is plotted in Fig. 2.

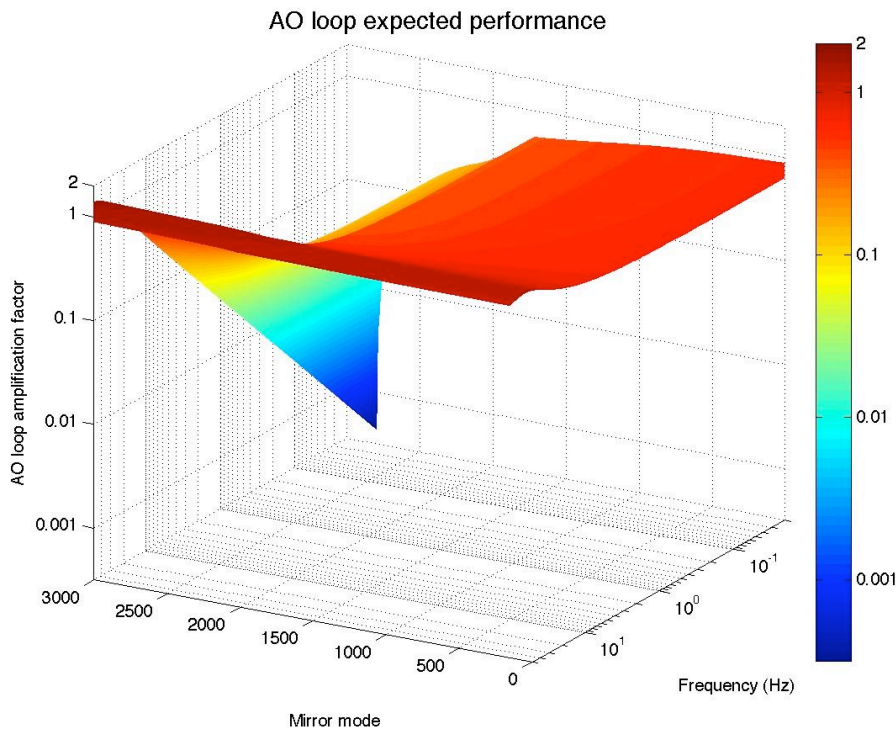


Fig. 2 AO rejection function

3. CONTROL STRATEGIES

3.1 Overview

From a dynamic control point of view the M1 figure control system can be represented as a MIMO system with a controller structure as shown in Fig. 3, where:

- G_{PTT} is the segmented mirror to be controlled,
- C_S is the controller matrix of the inner loop often used to adjust segment stiffness and damping based on local measurements (PACT displacement or segment acceleration). It is also used to isolate segments from vibrations of backstructure.
- IM is the interaction matrix from segment coordinates to edge sensor,
- CM is the control matrix to transform edge sensor measurements into segment coordinates,
- C_G is the ES loop controller.

The dynamical system to be controlled is represented by the transfer function matrix G_{PTT} . For a flexible backstructure this matrix is fully populated (inter-segment coupling).

For wind force rejection it is advantageous to have a high stiffness and damping on mirror level. Locally on segment level, the relative stiffness and damping between segment and backstructure can be adjusted to some extent by mechanical design or by an inner loop based on local measurements. For a flexible backstructure two main difficulties need to be addressed:

- The finite backstructure stiffness allows segment displacements even for locally stiff segments.
- Stiffening segments by an inner loop could lead to instabilities resp. performance degradation due to crosstalk.

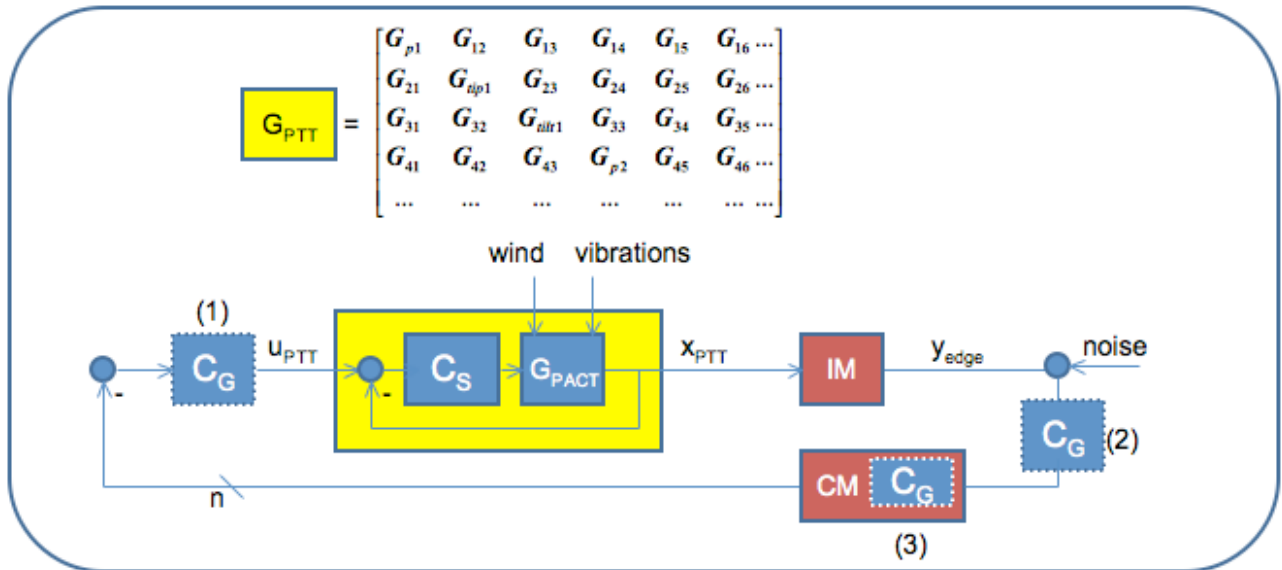


Fig. 3 M1 figure control system. Several locations of the controller matrix C_G are possible: global control: C_G at location (1), modal control: C_G at location (2) and local control: C_G at location (1) + CM modified

In this paper the first point is addressed. The M1 figure control is studied with flexible backstructure neglecting any inner loop. The PACT stiffness is adjusted by parameters in the mechanical model. In a future step, details about inner loop properties and the adjustment of the inner loop are investigated. Preliminary results considering segment piston only were already presented in [1].

3.2 Studied control strategies

For the M1 figure control, several strategies and thus several locations for the control matrix are possible. Their main difference is in the way the ES information is used to close the loop. Three approaches were studied:

Global control

In global control the PTT references (u_{PTT}) for each segment are computed from the projection of ES signals to segment coordinates. This approach seems to be optimal to minimize ES readings. However, the closed-loop bandwidth of individual mirror modes cannot be handled easily.

Modal control

In modal control the controller matrix is applied in mirror mode space, defined by the Singular Value Decomposition (SVD) of the PACT to ES IM. The control bandwidth can be adjusted mode by mode to balance optimally the noise propagation and the perturbation rejection. In order to allow different controller structures for each mode independently, the ES are first projected on mirror modes and the calculated controller command is projected further on segment coordinates. Therefore, the CM is split into 2 parts and the computational load is significantly larger than for global control.

Local control

Local control aims also at reducing the sensitivity of the control performance to edge sensor noise with the added benefit to decrease the computational load. For this purpose the control matrix CM is approximated in a way that for each segment only measurements of segments in its proximity are used to reconstruct its position error. Three different sizes of “segment islands” were studied: 1, 7 and 37 segments. Propagation of edge sensor failures is limited in range. However, cross talk between modes is increased by using only an approximation of the control matrix.

3.3 Baseline for M1 figure control loop

The three strategies introduced in the previous section were thoroughly studied. Modal control was selected as the baseline for the E-ELT M1 figure control for the following reasons:

Flexibility

In modal control, different controller dynamics can be applied for individual mirror modes or groups of mirror modes. Due to flexible backstructure, a few modes (mainly low spatial frequency modes) suffer from cross coupling (control structure interaction), whereas all other modes are practically decoupled. Using two groups of controllers avoids sacrificing bandwidths of the majority of modes for a few slow ones. This is one of the main drawbacks of global control, where the controllers are not mapped to mirror modes, but segment dynamics.

ES noise propagation

Some mirror modes are badly observable by ES. As a consequence ES noise has a very strong impact on these modes. The difference in noise level is more than 2 magnitudes. Noise propagation onto mirror modes is detailed in [2]. Modal control allows selecting the control bandwidth for each mirror mode independently and therefore reducing the impact of ES noise onto control performance. Local control incorporates a reduction of gains on the low spatial frequency modes by construction of the CM. However, the distribution of modal gains cannot be adjusted to optimize the performance and robustness of the system. Global control suffers from large noise propagation at low spatial frequency modes.

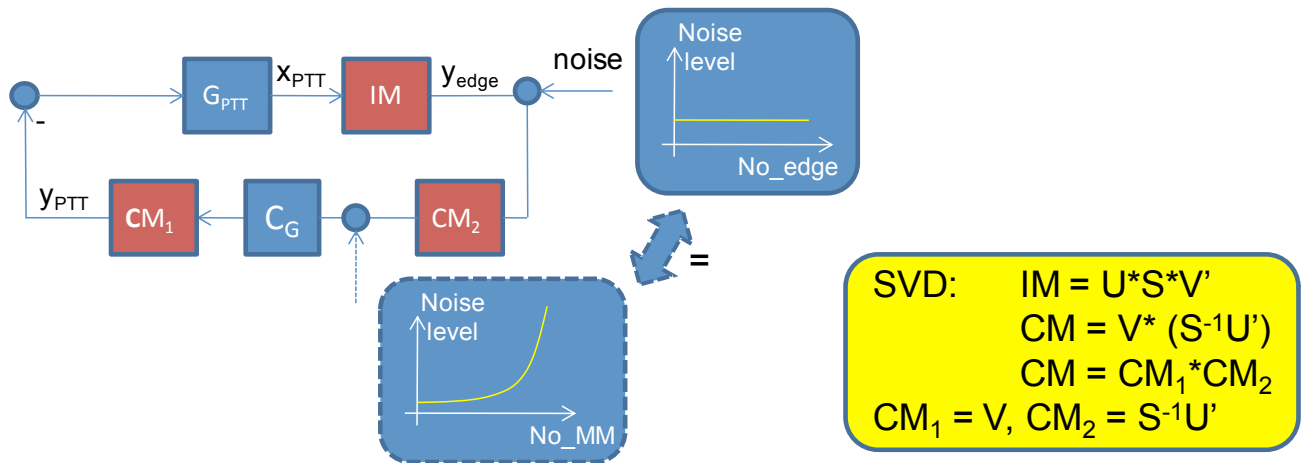


Fig. 4 Translation of ES noise onto noise on mirror modes. CM_2 and CM_1 are the transformation matrices from ES to SVD mirror modes and from SVD mirror modes to segment PTT, respectively.

M1 kernel control

Four mirror modes are unobservable by ES and several low spatial frequency modes suffer from poor observability. The non-observable modes correspond to global rigid body motions of M1 (i.e. global piston, tip and tilt) and change of radius of curvature (focus). The set of these modes need to be observed by other means, e.g. using the local PACT positions or the AO control system. Modal control allows to incorporate to the control of the M1 kernel in a straightforward manner.

3.4 Tradeoff of segment stiffness and ES loop bandwidth

Wind rejection in the context of M1 figure control can be established at least in two ways, either by locally stiffening the segments or by high bandwidth control on edge sensors. The former approach is usually preferred for several reasons. As mentioned above practically achievable ES control loop bandwidth is limited especially for low spatial frequency modes

because of noise propagation and control structure interaction. Additionally, by stiffening segments wind rejection is also improved for badly observable modes and thus telescope operations become simple.

For the M1 figure control the goal is to limit the ES loop bandwidth to a few Hz and to keep the controllers as simple and robust as possible. For this purpose the necessary segment stiffness was estimated with a simplified M1 model.

Each segment is modeled as a spring damper system with a relative damping of $D = 0.15$. Whiffle tree, PACT and framework structure stiffness are combined into one spring at each PACT location. The ES loop is assumed to have 2nd order characteristics (40 dB roll-off) with relative damping of $D = 0.7$ and the indicated ES loop bandwidth. All modes are controlled with identical bandwidth. The range of stiffness analyzed corresponds to the range of segment eigenfrequencies of 10-60 Hz (soft versus hard actuator). The AO characteristics of Fig. 2 are assumed.

Fig. 5 shows the tradeoff between segment stiffness and ES loop bandwidth to reach the required wavefront residual of 10nm after AO. As expected, it indicates that low segment stiffness induces large bandwidth requirements for the ES loop. In order to reach a residual 10 nm rms wavefront after AO with reasonable ES bandwidth, a segment stiffness of about 10N/μm is needed at each PACT location. For a whiffle tree stiffness of 17N/μm [4] and a framework structure stiffness of 100 N/μm [4] the resulting PACT stiffness has to be above 55 N/μm.

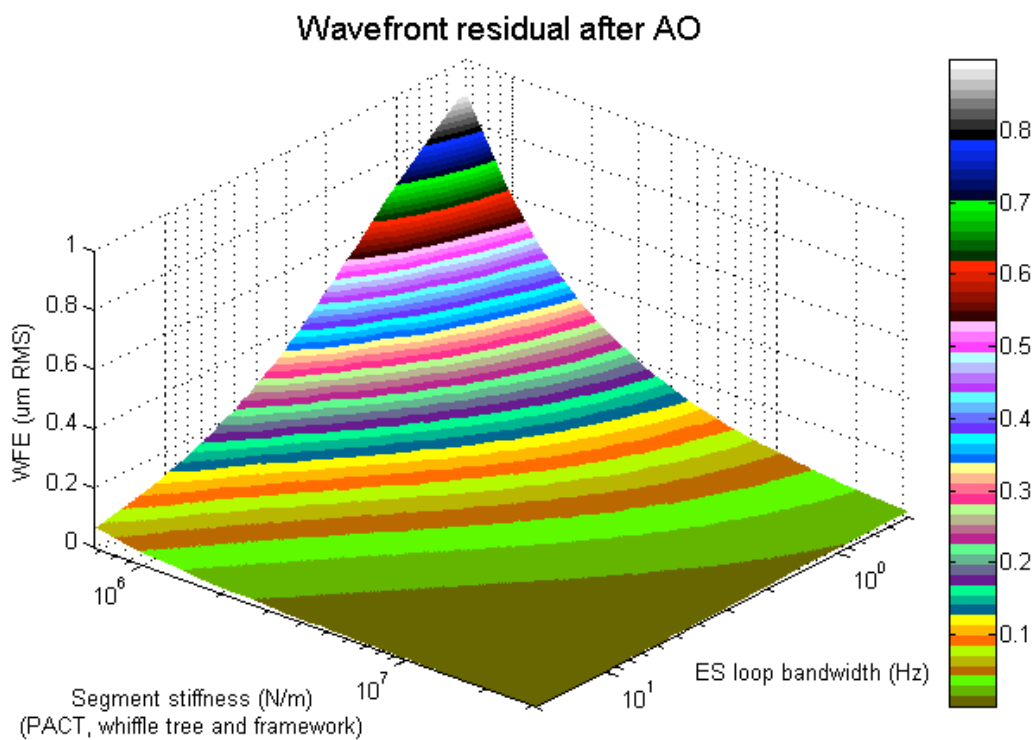


Fig. 5 Tradeoff between segment stiffness and ES loop bandwidth for wind rejection.

4. SIMULATIONS

The suitability of the baseline control strategy introduced in the previous sections was confirmed by time-domain simulations. A dynamical model of the ELT M1 was setup. Characteristic wind perturbations and an ES noise profile were generated. Modal controllers were designed and simulations were run for 60 seconds.

4.1 Dynamical model of the E-ELT M1 system

The M1 system is modeled in form of a finite element model. This model contains all necessary control and perturbation inputs (PACT and wind forces) and delivers segment positions in all degrees of freedom as output. The model contains about 10000 modes. It covers a frequency range of up to approximately 150 Hz. A modal damping of 0.75% is assumed. For the selected PACT stiffness of 57 N/ μm the main segment eigenfrequencies of a single segment are 76 Hz in piston and 56Hz in tip and tilt.

Intersegment edges are measured by ES located 5cm from segment vertices. Segment references and wind forces are expressed in PTT in order to reduce the dynamical coupling on segment level.

The backstructure is rather stiff concerning high spatial frequency modes. Therefore, high spatial frequency mirror modes are well represented by the segment dynamics, almost neglecting backstructure modes. However, lower spatial frequencies mirror modes tend to excite the backstructure because of the large segment inertia involved. Fig. 6 illustrates the split of modal transfer functions in spatial frequencies.

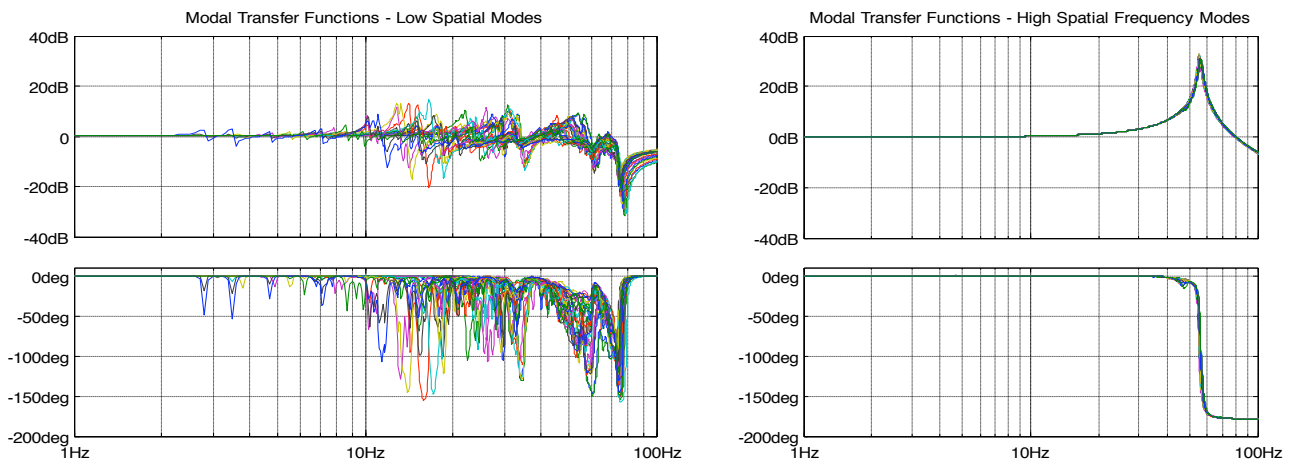


Fig. 6 Modal transfer functions. Mechanical modes of the backstructure print through for low spatial frequencies. High spatial frequencies are dominated by segment dynamics.

4.2 Controller Design

The modal controllers are designed with the objectives to provide good wind rejection, low ES noise propagation and good robustness in order to cope with the different modal transfer functions of Fig. 6 and the modal cross coupling due to flexible backstructure. The controller best suited for the listed objectives is a double integral controller with a lead-lag compensator of the form $C_G = K(s+b)/s^2(s+a)$. The closed-loop bandwidth was adjusted to about 2Hz. Zero and pole of the lead-lag were placed at the cross-over frequency (approximately 2Hz) and 30Hz, respectively, in order to provide enough phase margin in the region, where most of the modes are located. In addition, a mode filter in form of a simple gain scheduling was applied on the least observable modes (low spatial frequency) in order to reduce ES noise propagation into these modes. The controller has a 40dB roll-off at low frequency for wind rejection and provides a phase margin of more than 50deg for all modes. Note that for a large set of modes the closed loop bandwidth could be further increased. However, with the idealized assumptions considered so far 2Hz BW is fully sufficient.

4.3 Simulation Results

All simulations are run with a sampling frequency of 200Hz for duration of 60 seconds. Only the second half of the data is evaluated in order to avoid transient effects.

In Fig. 7 and Fig. 8 the results of the selected strategy are given. The residual before AO is concentrated into the very low spatial frequency modes that are badly controlled with ES. After AO these errors are reduced to a few nm wavefront rms. ES noise has no visible impact to the performance. No degradation of performance and stability due to modal cross-coupling was observed.

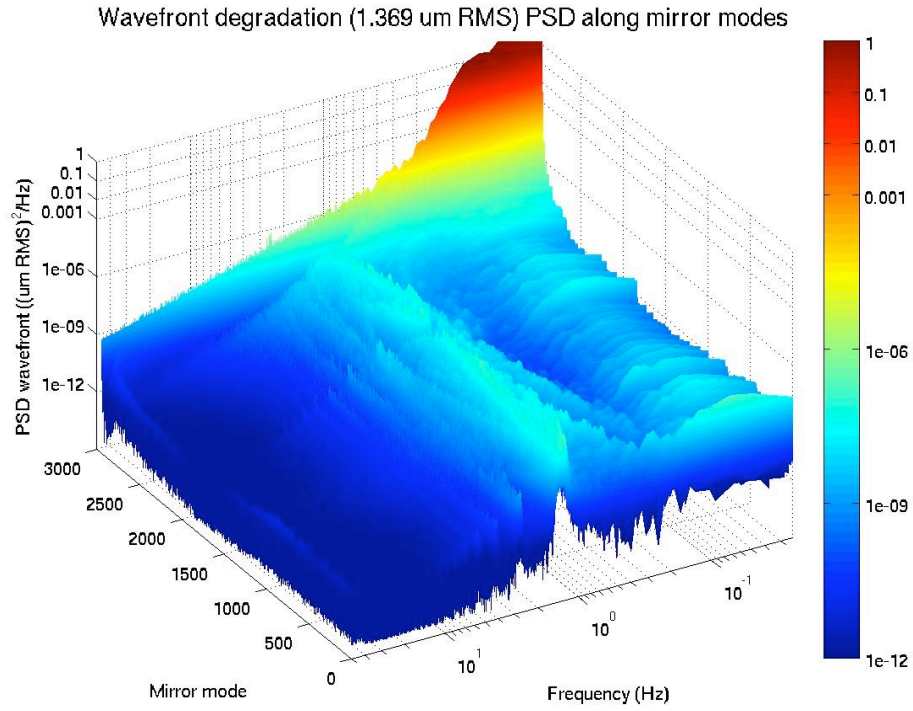


Fig. 7 PSD of the residual before AO Correction (low spatial frequency correspond to high mode numbers)

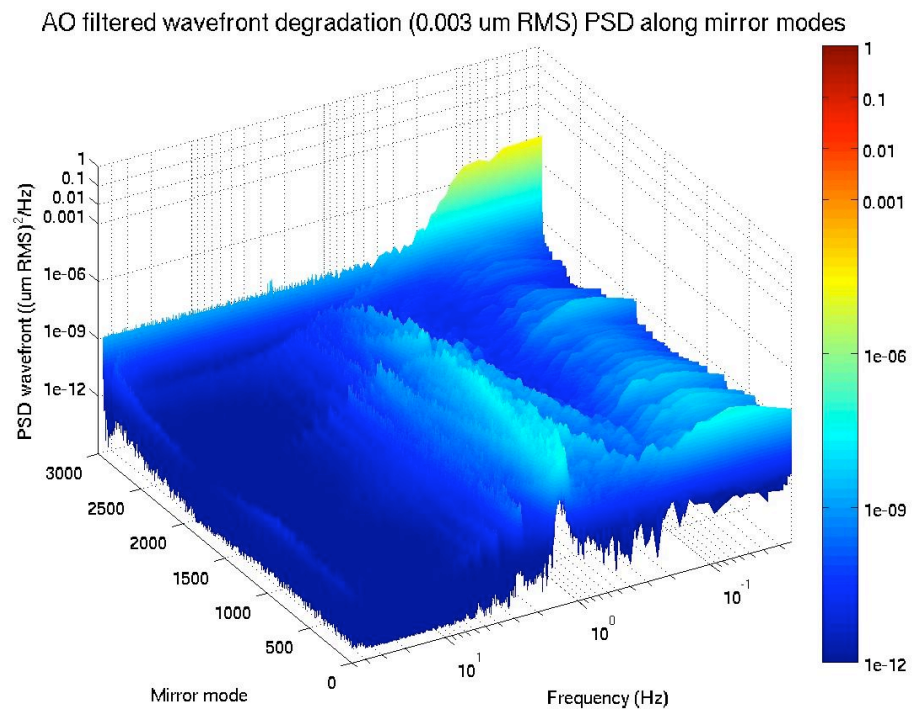


Fig. 8 PSD of the residual after AO Correction

4.4 Open issues and ongoing activities

Even though the baseline strategy of locally stiffening the segments and applying modal control for the ES loop fulfils the requirement of wavefront error after AO, several perturbations and numerical aspects were left out in this analysis. In this chapter areas are presented, which are addressed in ongoing or future works.

Influence of in-plane motions

ES are sensitive to inter-segment gap and shear variations due to quasi-static telescope deformations under changing gravity (during telescope tracking) and thermal conditions. The first order effect is a quasi-static drift of the ES signal that cannot be removed by the M1 figure control system. Since some of the modes affected are difficult to reject by AO, this might have an impact on the operational strategy (recalibration of ES with phasing sensor) or compensations at ES level using a Look-Up Table (LUT) or additional sensors. Work in this area is currently ongoing. An ES model was setup and the influence of gravity and thermal errors was studied. Without compensation the magnitude of the resulting wavefront errors is similar in amplitude to the wind induced errors (approximately $1.5 \mu\text{m}$ rms wavefront). The second order effect is a modification of the sensitivity of ES to segment PTT motions, resulting in a distortion of the IM.

Sensitivity to IM numerical errors

Numerical errors in the IM can cause modal crosstalk and reduce stability margins. Especially low spatial frequency modes will be affected, since they are badly observable from ES. This topic is closely related to changes of M1 geometry due to in-plane motions and mounting errors. No consolidated results are available so far, but work in this area is scheduled for second half of 2008.

M1 kernel control

The low spatial frequency modes suffer from bad observability with ES. At the moment several alternative strategies to control the M1 kernel, especially during telescope preset where no AO is available, are investigated (e.g. using PACT position sensors, reference segments, etc.).

Stability of PACT control loop

Depending on the choice of PACT (soft or hard actuator) and the requirements concerning blind segment positioning (without ES), closing an inner loop on a local PACT sensor with sufficient stiffness at low frequencies might be very difficult because of backstructure interaction. Inner loops with sufficient bandwidth and stiffness were already simulated for E-ELT segments using a quasi-SISO design method. However, work is still going on to understand better the limitations imposed by the flexible backstructure.

Vibration rejection

Stiffening segments on their support in order to improve wind rejection, might allow vibrations to be transmitted from the backstructure to the segments. As mentioned earlier, especially narrow-band vibrations are expected. Since vibration frequencies are typically in the 10Hz to 60Hz frequency region (VLTI experience), they cannot be rejected by the ES loop. The E-ELT project is not yet in a state to specify the vibration levels to be expected at the level of M1 segments. Work is going on to identify critical vibration sources and their transfer function through the telescope structure. At the moment two mitigation strategies are considered to isolate segments from narrow band vibrations.

Introducing notch filters allows opening the PACT loop at specific frequencies and thus lowering the backstructure-to-segment stiffness to the open loop actuator stiffness. For the vibration frequency range considered this method is only efficient for soft actuators.

Vibrations could be measured by load cells or accelerometers. The measurement is used to close a local feedback loop on the PACT or in a quasi open loop scheme by imposing an oscillation in opposite phase (and tracking its frequency and phase). The former is known as Acceleration Feedback Control (AFC) and is used to improve the wind rejection of telescope axes [5]. The latter is known as Vibration Tracking (VTK) and was successfully applied to suppress vibrations for fringe tracking in VLTI [6].

AO rejection

So far the assumption on AO rejection comes from a crude model assuming a linear response of the AO system to M1 control errors. Since it plays an important role for the estimation of post AO errors, in an ongoing activity the rejection

characteristics are simulated in more detail taking into account actuator patterns. Especially the dependency of AO rejection on M1 SVD modes and the limit of the linear response are investigated.

PACT sensor noise propagation

So far noise of PACT sensors (position and acceleration) was not considered. Work is going on especially in the area of defining requirements for blind offsetting of segments for ES calibration and coherenceing. Stringent requirements on sensor accuracy might have an important impact on PACT unit price.

5. IMPLEMENTATION

The objective for the implementation is to provide a cost effective way to achieve the functional and performance requirements of the Primary Mirror System. The goal is to operate the M1 figure control loop with a cycle time of 1ms to enable sampling and modeling vibrations located beyond the control loop bandwidth.

5.1 Primary mirror controls architecture overview

The baseline architecture is exploiting the six-fold symmetry of the segmented primary mirror and accordingly it is partitioned in to six identical groups of 164 segments.

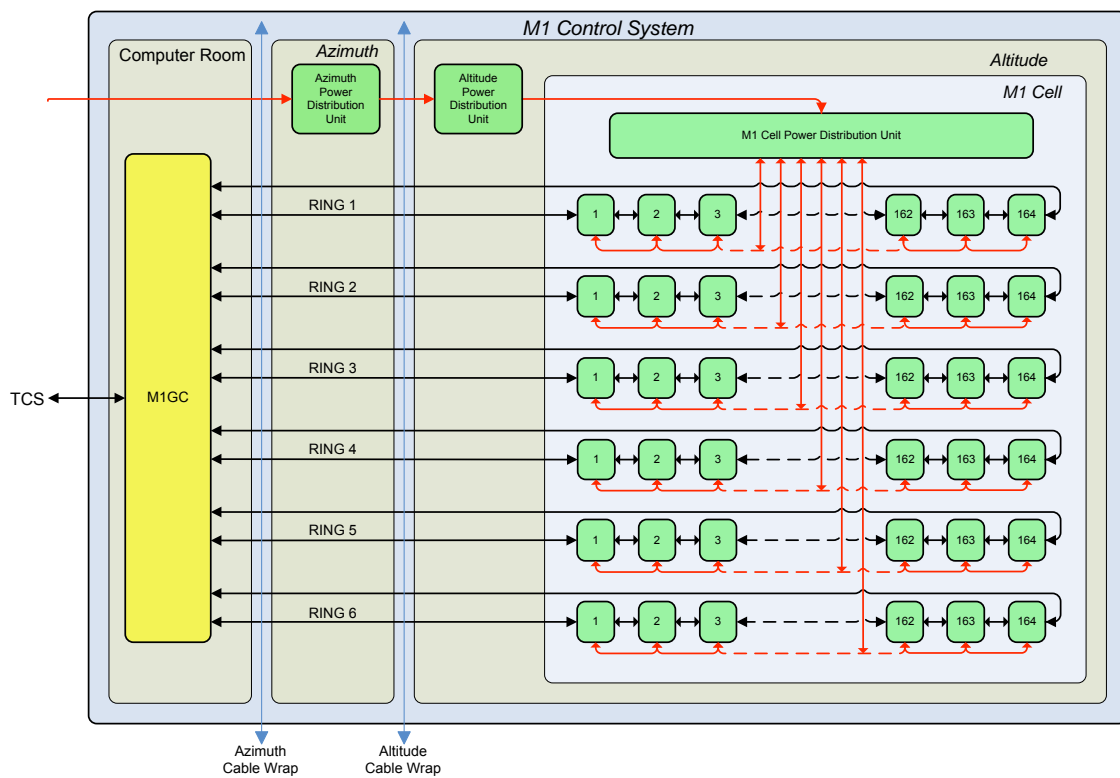


Fig. 9 M1 Control System architecture

5.2 High performance computing on multi-core architecture

The challenge for real-time control of large MIMO system does not only reside in the large number of computation associated to the solving of the linear problem but also in the amount of data that it represents. Pure computational power, memory management and data transfer are deeply coupled to determine the actual performance of the computing architecture; e.g. single-precision floating point representation operations are preferred in order to reduce the amount of cache memory required to store the large data set associated to the modal projection matrices.

Different architectures were analyzed and a cost effective solution was found using mainstream multi-core workstations. Benchmarks show that modal control algorithm can be implemented using LabVIEW and executed in 560us when deployed on 6 DELL T7400 dual quad-core workstations.

5.3 Communication

Communication between the segment concentrators and the MIGC can be built using six identical EtherCAT rings. The data requires an address range of 5.6kBytes on each EtherCAT ring and could therefore be transmitted using four full-size Ethernet frames.

EtherCAT is a deterministic protocol using 100Mb/s Ethernet physical layer and the ring topology offers some level of redundancy and automatic failure recovery. EtherCAT would introduce a communication delay between MIGC and the segment concentrators of about 300us.

5.4 Synchronization

The synchronization within each of the six parts of the communications network is ensured by EtherCAT to sub-microsecond accuracy. The global E-ELT Time Reference System (TRS) shall make use of the Precision Time Protocol [7] deployed on the Telescope Control Network. Synchronization between the six EtherCAT rings may be achieved by synchronizing the EtherCAT master clock of each ring to the TRS by means of an additional node connected to the telescope control network.

6. CONCLUSION

In this paper the progress in the area of E-ELT M1 figure control was summarized. Modal control with local stiffening of segments was selected as baseline for the edge sensor loop. Its main advantage compared to other strategies is its flexibility to optimize the dynamics of individual mirror modes. This fits well the needs to address different noise characteristics and sensitivities to backstructure for different mirror modes. The performance estimates were confirmed by E-ELT M1 system simulations considering ES noise and wind buffeting. The baseline strategy reached a residual below the specified value of 10 nm rms. The contribution from flexible backstructure is large before AO, but limited to slow low spatial frequency modes of the M1 kernel that can be efficiently removed by AO. For telescope preset a dedicated kernel control strategy is needed. Modal cross coupling was not a concern for the selected high M1 cell stiffness and low ES bandwidth. Lowering M1 cell stiffness will significantly reduce the performance margins.

Many details were still left out for this first evaluation of the ELT M1 figure control. The open points have been identified and the planned/ongoing work was reported.

A possible architecture for the implementation of the modal control baseline was presented. The necessary tests were done on a hardware demonstrator. The proposed architecture could be implemented with Commercial Off-the-shelf hardware available today.

REFERENCES

- [1] Sedghi, B., Miskovic, M., Dimmler, M., "Perturbation Rejection Control Strategy for OWL," Proc. SPIE 6271, 0L1-0L12 (2006).
- [2] Chanan, G., MacMartin, D. G., Nelson, J., and Mast, T., "Control and alignment of segmented-mirror telescopes: matrices, modes, and error propagation," Applied Optics Vol. 43, No.6 (2004).
- [3] MacMartin, D. G. and Chanan, G., "Control of the California Extremely Large Telescope Primary Mirror," Proc. SPIE 4840, 69-80 (2002).
- [4] Cavaller, L., Marrero, J., Castro, J., Ronquillo, M., Hernandez, E., "Design of the primary mirror segment support system for the E-ELT," Proc. SPIE 7012 (2008).
- [5] Sedghi, B., Bauvir, B. and Dimmler, M., "Acceleration Feedback Control on an AT," Proc. SPIE 7012 (2008).
- [6] Di Lieto, N., Hagenauer, P., Sahlmann, J., Vasisht, G., "Adaptive Vibration Cancellation on Large Telescopes for Stellar Interferometry," Proc. SPIE 7012 (2008).
- [7] Eidson, John C., [Measurement, Control and Communication Using IEEE 1588], Springer, London (2006).